AGU PUBLICATIONS

Geophysical Research Letters

RESEARCH LETTER

10.1002/2013GL058745

Key Points:
- Blocking has not exhibited positive trends over the last 15–30 years
- Blocking shows large interannual and decadal variability
- No observed link between Arctic sea ice loss and blocking frequency

Supporting Information:
- Readme
- Barnes_etal_2014_GRL_Supplementary_Materials

Correspondence to:
E. A. Barnes,
eabarnes@atmos.colostate.edu

Citation:
Barnes, E. A., E. Dunn-Sigouin, G. Masato, and T. Woollings (2014), Exploring recent trends in Northern Hemisphere blocking, *Geophys. Res. Lett.*, *41*, doi:10.1002/2013GL058745.

Received 17 NOV 2013
Accepted 6 JAN 2014
Accepted article online 10 JAN 2014

Exploring recent trends in Northern Hemisphere blocking

Elizabeth A. Barnes[1], Etienne Dunn-Sigouin[2], Giacomo Masato[3], and Tim Woollings[4]

[1]Department of Atmospheric Science, Colorado State University, Fort Collins, Colorado, USA, [2]Department of Earth and Environmental Science and Lamont-Doherty Earth Observatory, Columbia University, New York, New York, USA, [3]Department of Meteorology, University of Reading, Reading, UK, [4]Atmospheric, Oceanic and Planetary Physics, University of Oxford, Oxford, UK

Abstract Observed blocking trends are diagnosed to test the hypothesis that recent Arctic warming and sea ice loss has increased the likelihood of blocking over the Northern Hemisphere. To ensure robust results, we diagnose blocking using three unique blocking identification methods from the literature, each applied to four different reanalyses. No clear hemispheric increase in blocking is found for any blocking index, and while seasonal increases and decreases are found for specific isolated regions and time periods, there is no instance where all three methods agree on a robust trend. Blocking is shown to exhibit large interannual and decadal variability, highlighting the difficulty in separating any potentially forced response from natural variability.

1. Introduction

Over the past two decades, the Arctic has experienced unprecedented sea ice loss [*National Snow and Ice Data Center*, 2013]. Recent studies suggest that the recent decline in sea ice has led to an increase in blocking over North America and Europe in all seasons but spring [e.g., *Liu et al.*, 2012; *Francis and Vavrus*, 2012] due to a slow down of the large-scale flow in response to the reduced lower tropospheric temperature gradient. Blocking is strongly tied to weather extremes in the midlatitudes (e.g., cold snaps, heat waves) and can persist for days to weeks [e.g., *Black et al.*, 2004; *Dole et al.*, 2011], so an increase in blocking could mean an increase in weather extremes as Arctic sea ice continues to decline. However, both observational and modeling studies suggest that any potential link between sea ice and midlatitude weather may be masked by internal variability [e.g., *Barnes*, 2013; *Screen et al.*, 2013]. Here we address whether robust trends in blocking have been observed over the past few decades in response to the hypothesis that recent Arctic sea ice loss has increased the likelihood of blocking over the Northern Hemisphere.

While a handful of previous studies have published trends in blocking [e.g., *Barnes*, 2013; *Croci-Maspoli et al.*, 2007], there is concern over whether the results are sensitive to the specific blocking detection algorithm employed, the data set used, or the season and time period over which the trend is defined. For this reason, we analyze blocking occurrence with three different detection methods, four different reanalyses, over all four seasons and three different year ranges. Our goal is to quantify whether blocking frequencies have in fact changed over the satellite era in an effort to (1) advance the discussion of the effects of Arctic change on midlatitude weather and (2) evaluate whether trends in blocking have been observed, regardless of the sea ice hypothesis, e.g., associated with the Atlantic Meridional Overturning circulation, or global temperature increases.

2. Data and Methods

2.1. Data

We compare blocking frequencies derived from four different reanalyses. Specifically, we use daily mean 500 hPa geopotential height (Z500) over the period 1980–2012 from the European Centre for Medium-Range Weather Forecasts's ERA-Interim Re-Analysis (ERA-I) [*Dee et al.*, 2011], NASA's Modern Era Reanalysis for Research and Applications (MERRA) reanalysis [*Rienecker et al.*, 2011], National Centers for Environmental Prediction/National Center for Atmospheric Research (NCEP/NCAR) Reanalysis [*Kalnay et al.*, 1996], and the NCEP-Department of Energy Reanalysis 2 (NCEP2) [*Kanamitsu et al.*, 2002]. Additional analysis is presented for the period 1948–2012 from NCEP. September Arctic sea ice extent was obtained from the *National Snow and Ice Data Center (NSIDC)* [2013] for 1979–2013.

2.2. Blocking Indices

Different blocking detection algorithms are designed to detect various aspects of a block throughout its lifetime, thus, we apply three different blocking indices to each of the four reanalyses to ensure that we diagnose trends with a range of possible blocking measures. The first blocking index follows *Barnes et al.* [2012] (B1D hereafter) and is a 1-D blocking index that searches for a persistent reversal of the meridional Z500 gradient along the latitude of the storm track, and thus, B1D is a function of longitude alone. The second blocking index follows *Dunn-Sigouin et al.* [2013] (D2D hereafter) and is a 2-D index that searches for persistent contiguous areas of geopotential height anomalies that occur in conjunction with reversals of Z500. The third blocking index is similar to B1D, except it is a 2-D index, searching for persistent large-scale reversals of the Z500 field associated with blocking and synoptic Rossby wave-breaking events (hereafter M2D) following *Masato et al.* [2013]. We refer the reader to the supporting information for additional details on the indices. Previous studies have confirmed that similar blocking statistics are obtained when blocking is identified using fields other than Z500 [e.g., *Barnes et al.*, 2012], and so we present results for Z500 only. Our goal is to determine whether robust trends in blocking have been observed in recent decades. For this reason, we do not present a blocking index intercomparison here, but rather, we view the three indices as equally valid, each capturing different aspects of blocking flow over the Northern Hemisphere.

2.3. Analysis Methods

Blocking frequencies for all three indices are defined as the number of days per month that a sector is part of a blocking event. We have also performed the analysis for the frequency of unique blocking onset days (one count per block), and the results will be discussed in the text. Blocking frequencies are binned as the monthly average blocking frequency in every 20° latitude by 60° longitude sector unless otherwise noted. For the time series analysis, the 40°–60°N and 60°–80°N sectors were averaged together to obtain the middle-to-high-latitude blocking frequencies as functions of longitude only.

Trends are calculated using linear least squares regression, and trends significantly different from zero are identified using a symmetric, two-tailed 95% confidence interval. We define sectors with *robust* trends as regions where at least 3 out of 4 of the reanalyses exhibit statistically significant trends of the same sign. To determine the significance of blocking differences between the five lowest and highest September sea ice years, we employ a bootstrap approach where 10,000 random sets of the same length are simulated and the 95% confidence interval is determined from the synthetic data.

3. Results

3.1. Blocking Climatology

Figure 1 displays the seasonal-mean blocking frequency climatologies. For ease of comparison, we have plotted the B1D frequencies at 45°N since this index provides blocking frequencies as a function of longitude only. The number of blocks per month differs among the indices due to the different criteria used to define a block. However, qualitatively, all three indices exhibit similar regional distributions. Blocking is most frequent in winter and is located predominantly over two main regions: the North Atlantic/Europe and the North Pacific. The red (blue) boxes denote sectors where robust increases (decreases) in blocking frequency are found between 1990 and 2012, as will be discussed.

3.2. Linear Trends

Blocking trends are shown in Figures 2a and 2b for two different periods as a function of longitude, season, and blocking index. Boxes are filled red (blue) if robust increases (decreases) in blocking frequency are observed over the period in either latitude band (40°–60°N or 60°–80°N). Note that there is no instance where both latitude ranges exhibit robust trends at the same time. We present trends over 1980–2012 and over the more recent 1990–2012 period, when previous studies suggest sea ice loss and Arctic warming have had the largest impact on the midlatitude circulation [e.g., *Francis and Vavrus*, 2012].

Focusing first on 1980–2012 trends (Figure 2a), no sector exhibits robust trends except the M2D index in June-July-August (JJA) over the North Atlantic (300°–360°E). When the period 1990–2012 is analyzed instead (Figure 2b), the North Atlantic no longer exhibits robust increases, and the 2-D indices show increases in blocking over Asia (60°–120°E) in December-January-February (DJF). A robust decrease in B1D blocking is observed over the Pacific (180°–240°E) in JJA. Note that no robust trends in blocking are identified in Autumn (September-October-November (SON)), the season when the sea ice trends are

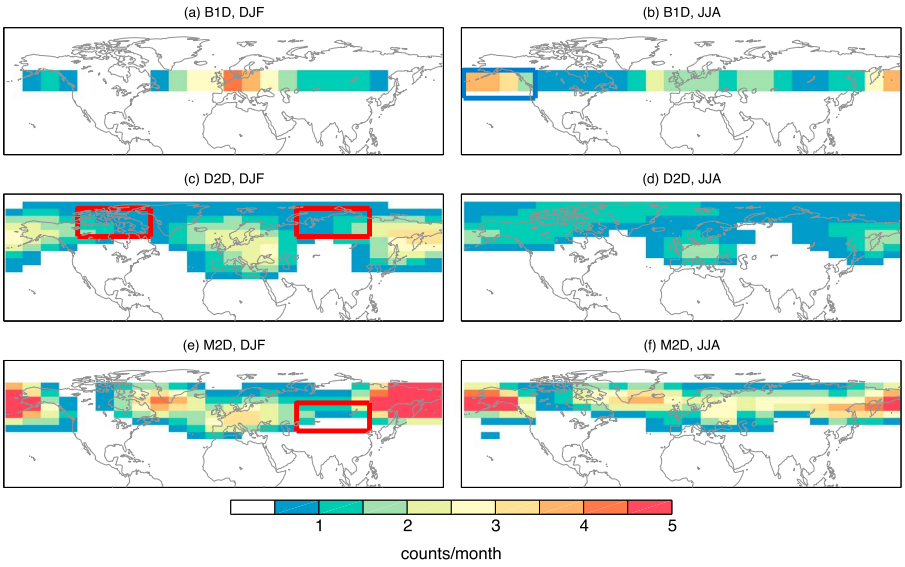

Figure 1. Climatological seasonal blocking frequency for the three indices using the MERRA reanalysis from 1980 to 2012. Red (blue) boxes denote regions where robust increases (decreases) in blocking frequency are found over the 1990–2012 period, as shown in Figure 2b.

the strongest [*National Snow and Ice Data Center (NSIDC)*, 2013]. If one analyzes the period 1995–2012, a robust negative trend is found in SON, and only Asia has a robust positive trend in DJF (Figure S1 in the supporting information).

The key result of Figures 2a and 2b is that no general increase in blocking over the Northern Hemisphere is observed, and the sectors, seasons and indices with robust trends vary depending on the years analyzed. Furthermore, even fewer robust increases are found if one analyzes blocking *onset* frequency (rather than total days blocked; Figure S2 in the supporting information).

We take a moment to discuss the probability of finding significant trends by chance. For any single reanalysis and index, basic Poisson statistics show that the expected number of sectors exhibiting significant trends *by chance* is 2.4 for the 2-D indices (48 "trials"; 2 latitude bins × 6 longitude bins × 4 seasons = 48), with a 95% confidence interval of between 0 and 5. For the 1-D index, there are only 24 "trials", and this leads to an expected number of false positives of 1.2 with a 95% confidence interval of between 0 and 3. In other words, for a given reanalysis and index, we expect up to 5 sectors to show robust trends by chance alone. We see from Figures 2a and 2b that none of the three indices have more than 3 sectors with robust trends.

Time series of blocking frequencies for the robust trends in Figures 2a and 2b are shown in Figure 3, specifically, for Asia (DJF) and the North Atlantic (JJA) for 1990–2012 and 1980–2012, respectively. Time series for Europe and North America are provided in Figures S3 and S4 in the supporting information. Asterisks in the legend denote reanalyses with significant trends over the period denoted by the best fit lines. Comparing Figures 2a, 2b, and 3, we see that the winter increases in blocking over Asia appear in two or more reanalyses for all three indices. However, over the North Atlantic in JJA, while M2D exhibits robust trends in blocking frequency (Figures 2a and 3f), the B1D and D2D indices do not exhibit significant trends for any of the reanalyses (Figures 3b and 3d). Figure 3 also demonstrates the large amount of interannual variability in blocking, and this is further supported by the fact that the standard deviation of blocking frequency can exceed 3 times the mean (Figure S5 in the supporting information).

While differences across indices are to be expected, the differences among the reanalyses for a given index may be surprising. For example, the D2D MERRA frequencies (Figures 3c and 3d) exhibit very different values than the other three reanalyses. Similarly, the M2D ERA-Interim frequencies also differ from the other three reanalyses over Asia (Figure 3e). This suggests that studies using different reanalysis products could disagree on "observed" trends in blocking, even if the same blocking identification method is employed.

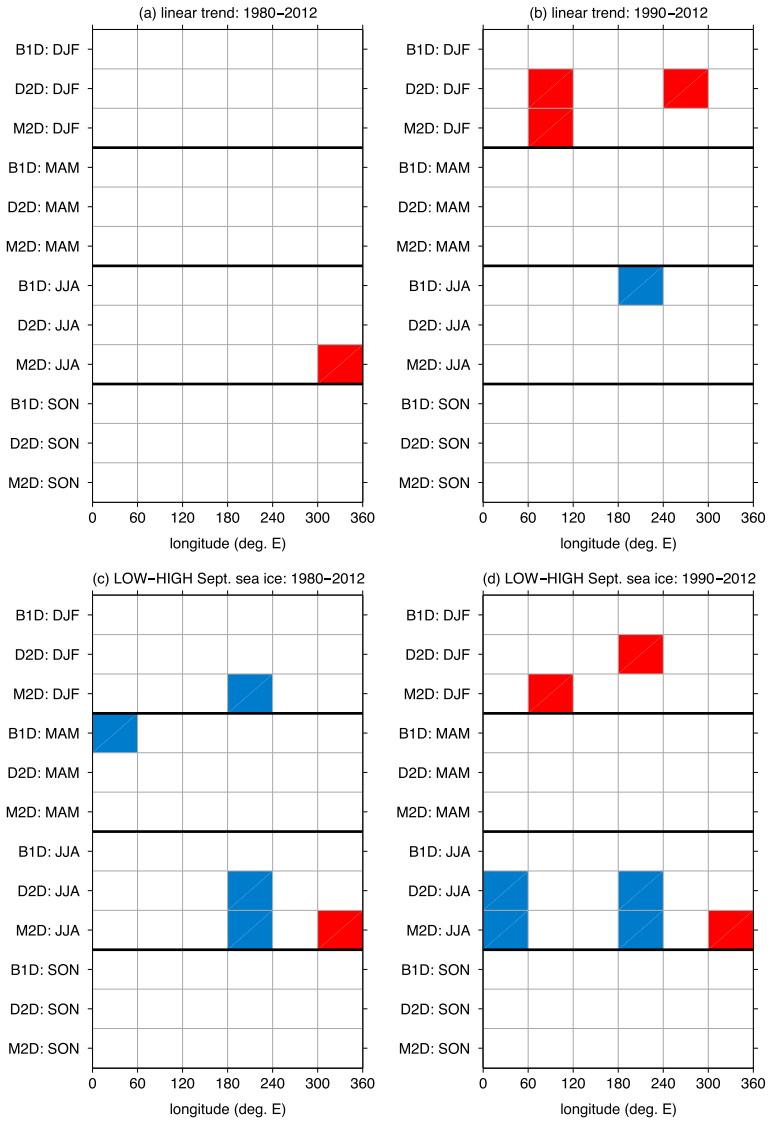

Figure 2. (a and b) Trends in blocking frequency between as a function of season, index, and longitude and (c and d) the difference in blocking frequency for seasons *following* the 5 September with the highest and lowest Arctic sea ice extent for (Figures 2a and 2c) 1980–2012 and (Figures 2b and 2d) 1990–2012. Red (blue) denotes that at least three of the four reanalyses exhibit statistically significant positive (negative) trends/differences at 95% confidence. For the 2-D indices, blocking trends are significant if either of the latitude bins (40°–60°N or 60°–80°N) show robust changes.

3.3. Sea Ice Composites

Robust differences in blocking for the seasons *following* the five lowest minus the five highest ice years are shown in Figures 2c and 2d (refer to Figure S6 in the supporting information for a time series of September sea ice extents). If low Arctic sea ice years have more blocking than high sea ice years, we expect positive differences in blocking (red colors) no matter the time period analyzed. However, both positive and negative differences are found in DJF (Figures 2c and 2d). Only JJA blocking for M2D over the North Atlantic (300°–360°E) exhibits significant positive differences over both periods, although this implies that low September sea ice precedes increased summer blocking by 9 to 12 months.

We strongly caution that composite differences, such as those in Figures 2c and 2d, should not be simply interpreted as the actual response of blocking to September sea ice anomalies. Sea ice extents were largest at the beginning of the time period (1980/1990s) and smallest at the end (2000s), and thus, any signal that oscillated over this period will produce a robust response even if it is independent of sea ice. For example, the winter North Atlantic Oscillation (NAO) transitioned from a positive to negative between the 1980/1990s and the 2000s [e.g., *Dong et al.*, 2011], and the negative NAO is strongly coupled to enhanced blocking

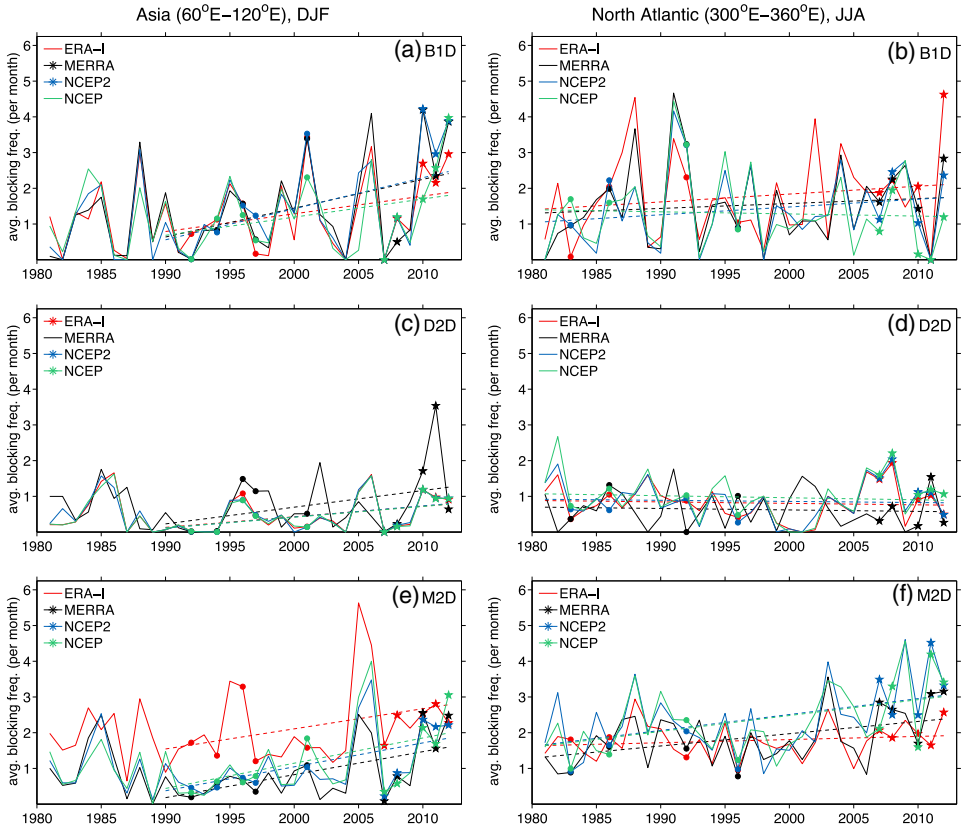

Figure 3. Time series of blocking frequencies for the three indices and four reanalyses for (a, c, and e) Asia in DJF and (b, d, and f) the North Atlantic in JJA. Trends significantly different from zero at 95% confidence are denoted by asterisks in the legend of each panel for Asia (1990–2012) and the North Atlantic (1980–2012). Filled circles (stars) denote the seasons *following* the 5 highest (lowest) years of September Arctic sea ice extent over the trend period. Blocking frequencies are averaged between 40° and 80°N for the 2-D indices.

in winter over the North Atlantic [e.g., *Davini et al.*, 2012]. Thus, the positive winter differences shown in Figure 2d could be associated with this low-frequency variability and not sea ice loss. On the other hand, modeling studies have shown that reduced Arctic sea ice can force the NAO into a negative state [e.g., *Deser et al.*, 2010] in winter, in which case, the DJF differences may represent a physical mechanism. However, circulation anomalies such as the NAO or blocking can also have a strong influence on Arctic sea ice [e.g., *Hu et al.*, 2002], making it difficult to disentangle cause and effect.

Liu et al. [2012] and *Tang et al.* [2013] use regression analysis to suggest that blocking frequencies have increased with recent sea ice loss, which disagrees with the results presented here. One possible explanation is the index used—they identify a block by persistent Z500 *anomalies* which can be influenced by large-scale changes in the Z500 field (e.g., by the general increase in Z500 due to high-latitude warming over the last decade). Our indices avoid this potential issue by requiring a reversal of the full Z500 field which equates to easterly winds and likely irreversibly deformed flow contours.

3.4. Decadal Variability

Finally, we place the prior analysis in a more historical context by including time series of NCEP blocking going back to 1948 (Figure 4). Blocking over all regions and seasons exhibits large decadal variability, with indices agreeing for some regions and seasons (e.g., North Atlantic, DJF), but not for others (e.g., Europe, JJA). In all sectors, blocking frequencies over the last few years do not appear exceptional in the context of the last sixty, and Figure 4 demonstrates the large amount of internal variability of blocking over the Northern Hemisphere on a range of time scales.

4. Conclusions

Recent studies have suggested that Arctic warming and sea ice loss over the past 15 years has led to an increase in the occurrence of blocking over the Northern Hemisphere [e.g., *Liu et al.*, 2012; *Francis and*

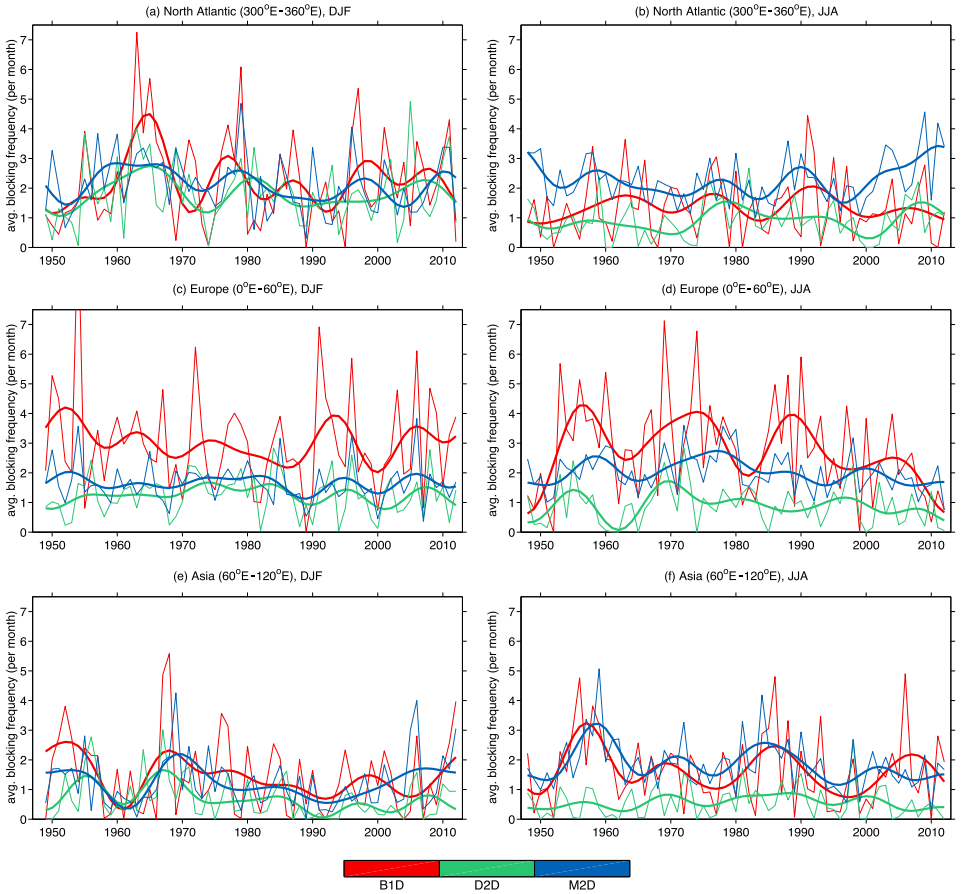

Figure 4. (a, c, and e) DJF and (b, d, and f) JJA blocking frequencies over three different sectors for the three indices using NCEP reanalysis from 1948 to 2012. Thick lines denote the smoothed time series using a Lanczos filter with 41 weights and a cutoff of 10 years. Blocking frequencies are averaged between 40° and 80°N for the 2-D indices.

Vavrus, 2012; *Tang et al.*, 2013]. We address whether blocking frequencies have exhibited robust trends in recent decades by applying three different blocking identification methods to four different reanalyses. No clear hemispheric increase in blocking is evident in any season for any blocking index, although robust seasonal increases and decreases are found for isolated regions. Compositing winter blocking frequencies on high and low September sea ice years yields opposite-signed differences depending on the years analyzed, while summer blocking yields positive differences over the North Atlantic and negative over the North Pacific. We strongly caution, however, that these composite differences can be explained by many different dynamical mechanisms and should not be simply viewed as evidence of the response of blocking to sea ice loss.

These conclusions support those of *Barnes* [2013], namely, that the link between recent Arctic warming and increased Northern Hemisphere blocking is currently not supported by observations. While Arctic sea ice experienced unprecedented losses in recent years, blocking frequencies in these years do not appear exceptional, falling well within their historically observed range. The large variability of blocking occurrence, on both internannual and decadal time scales, underscores the difficulty in separating any potentially forced response from natural variability.

Acknowledgments
The authors thank James Screen and an anonymous reviewer for their helpful comments on a previous version of the manuscript.

The Editor thanks James Screen and an anonymous reviewer for their assistance in evaluating this paper.

References

Barnes, E. A. (2013), Revisiting the evidence linking Arctic amplification to extreme weather in midlatitudes, *Geophys. Res. Lett.*, *40*, 4728–4733, doi:10.1002/grl.50880.

Barnes, E. A., J. Slingo, and T. Woollings (2012), A methodology for the comparison of blocking climatologies across indices, models and climate scenarios, *Clim. Dyn.*, *38*, 2467–2481.

Black, E., M. Blackburn, G. Harrison, B. Hoskins, and J. Methven (2004), Factors contributing to the summer 2003 European heatwave, *Weather*, *17*, 4080–4088.

Croci-Maspoli, M., C. Schwierz, and H. C. Davies (2007), A multifaceted climatology of atmospheric blocking and its recent linear trend, *J. Climate*, *20*, 633–649.

Davini, P., C. Cagnazzo, R. Neale, and J. Tribbia (2012), Coupling between Greenland blocking and the North Atlantic Oscillation pattern, *Geophys. Res. Lett.*, *39*(14), L14701, doi:10.1029/2012GL052315.

Dee, D. P., et al. (2011), The ERA-Interim reanalysis: Configuration and performance of the data assimilation system, *Q. J. R. Meteorolog. Soc.*, *137*(656), 553–597.

Deser, C., R. Tomas, M. Alexander, and D. Lawrence (2010), The seasonal atmospheric response to projected arctic sea ice loss in the late twenty-first century, *J. Climate*, *23*(2), 333–351.

Dole, R., et al. (2011), Was there a basis for anticipating the 2010 Russian heat wave?, *Geophys. Res. Lett.*, *38*, L06702, doi:10.1029/2010GL046582.

Dong, B., R. T. Sutton, and T. Woollings (2011), Changes of interannual NAO variability in response to greenhouse gases forcing, *Clim. Dyn.*, *37*(7-8), 1621–1641.

Dunn-Sigouin, E., S.-W. Son, and H. Lin (2013), Evaluation of Northern Hemisphere blocking climatology in the Global Environment Multiscale (GEM) model, *Mon. Weather Rev.*, *141*, 707–727.

Francis, J. A., and S. J. Vavrus (2012), Evidence linking Arctic amplification to extreme weather in mid-latitudes, *Geophys. Res. Lett.*, *39*(6), L06801, doi:10.1029/2012GL051000.

Hu, A., C. Rooth, R. Bleck, and C. Deser (2002), NAO influence on sea ice extent in the Eurasian coastal region, *Geophys. Res. Lett.*, *29*(22), 2053, doi:10.1029/2001GL014293.

Kalnay, E., et al. (1996), The NCEP/NCAR 40-year reanalysis project, *Bull. Am. Meteorol. Soc.*, *83*, 437–471.

Kanamitsu, M., W. Ebisuzaki, J. Woollen, S.-K. Yang, J. Hnilo, M. Fiorino, and G. L. Potter (2002), NCEP-DEO AMIP-II Reanalysis (R-2), *Bull. Am. Meteorol. Soc.*, *24*, 1631–1643.

Liu, J., J. Curry, and H. Wang (2012), Impact of declining Arctic sea ice on winter snowfall, *Proc. Natl. Acad. Sci. U.S.A.*, *109*(11), 4074–4079.

Masato, G., B. J. Hoskins, and T. J. Woolings (2013), Winter and Summer Northern Hemisphere blocking in CMIP5 models, *J. Clim.*, *26*, 7044–7059, doi:10.1175/JCLI-D-12-00466.1.

National Snow and Ice Data Center (NSIDC) (2013), National Snow and Ice Data Center, http://nsidc.org.

Rienecker, M. M., et al. (2011), MERRA: NASA's modern-era retrospective analysis for research and applications, *J. Clim.*, *24*, 3624–3648.

Screen, J., C. Deser, I. Simmonds, and R. Tomas (2013), Atmospheric impacts of Arctic sea-ice loss, 1979-2009: Separating forced change from atmospheric internal variability, *Clim. Dyn.*, doi:10.1007/s00382-013-1830-9.

Tang, Q., X. Zhang, X. Yang, and J. A. Francis (2013), Cold winter extremes in northern continents linked to Arctic sea ice loss, *Environ. Res. Lett.*, *8*(1), 014,036, doi:10.1088/1748-9326/8/1/014036.